Oceanologia (2018) 60, 232—243

Available online at www.sciencedirect.com

ScienceDirect

journal homepage: www.journals.elsevier.com/oceanologia/

ORIGINAL RESEARCH ARTICLE

Galveston Bay dynamics under different wind conditions

David Salas-Monreal [a,*], Ayal Anis [b], David Alberto Salas-de-Leon [c]

[a] *Universidad Veracruzana, Boca del Rio, Mexico*
[b] *Texas A&M University, Galveston, USA*
[c] *National Autonomous University of Mexico (UNAM), Ciudad Universitaria, Mexico City, Mexico*

Received 25 May 2017; accepted 17 October 2017
Available online 6 November 2017

KEYWORDS
Suspended particle dispersion;
Shallow estuarine dynamics;
Galveston Bay dynamics;
Ocean shallow water gyres

Summary The Regional Ocean Model System (ROMS) was used to simulate flow and hydrographic (temperature, salinity) patterns in a shallow, relatively flat-bottomed estuary with two subestuaries, one with an elongated shape and the other with a roughly circular shape. Simulations were used to elucidate the wind stress effect on a tidally formed cyclonic gyre in Galveston Bay, Texas (USA). The form factor suggests that Galveston Bay is a mixed, mainly diurnal system with tides that propagate out of phase by less than 1 h from side to side of the estuary. Temperature and salinity patterns suggest that the influence of the estuary extends oceanward, up to a distance commensurate with the 14 m depth isobath (~10 km offshore), during a diurnal tidal cycle. A tidally generated cyclonic gyre was observed to form in the circular subestuary, suggesting that this region may be more productive than others. This tidally formed gyre appeared to weaken and even disappear under certain wind stress conditions. Simulations suggest that the entire bay was able to flush only under northeasterly wind conditions, while for all other wind directions (northwesterly, southeasterly and southwesterly), the water appeared to pile up in the circular subestuary. Furthermore, most of the ocean-bay exchange was found to occur through the north entrance to the bay where the effects of the gyre were observed. Thus, it is expected that much of the exchange of water-borne substances, pollutants and plankton between the bay and the ocean occurs through this entrance.
© 2017 Institute of Oceanology of the Polish Academy of Sciences. Production and hosting by Elsevier Sp. z o.o. This is an open access article under the CC BY-NC-ND license (http://creativecommons.org/licenses/by-nc-nd/4.0/).

* Corresponding author at: Calle Hidalgo #617, Boca del Rio, Veracruz 94290, Mexico. Tel.: +52 229 9567070.
E-mail address: davsalas@uv.mx (D. Salas-Monreal).
Peer review under the responsibility of Institute of Oceanology of the Polish Academy of Sciences.

https://doi.org/10.1016/j.oceano.2017.10.005
0078-3234/© 2017 Institute of Oceanology of the Polish Academy of Sciences. Production and hosting by Elsevier Sp. z o.o. This is an open access article under the CC BY-NC-ND license (http://creativecommons.org/licenses/by-nc-nd/4.0/).

1. Introduction

Coastal marine ecosystems areas have been studied to understand sediment transport (Agardy, 2000; Salas-Monreal et al., 2009), zooplankton dispersion (Becerro et al., 2006; Chacon-Gomez et al., 2013; Holliday and Pieper, 1980) and the spatial and temporal variability of hydrodynamics and currents (Avendaño-Alvarez et al., 2017; Goreau and Hayes, 1994; Salas-de-Leon et al., 2004a; Wilkinson and Souter, 2008). In estuaries, gyres are commonly generated by current rectification (Storlazzi et al., 2006) due to the coastal boundaries. These gyres are one of the most important factors affecting the distribution of productive areas, sedimentation, vertical water movements, pollutants, and suspended matter concentrations (Salas-Monreal et al., 2009). Cyclonic gyres have been shown to generate highly productive areas by pumping deeper, high-nutrient, cold waters to the surface in the open ocean (Salas-de-León et al., 2008); however, in shallow waters the effects of gyres have not yet been fully described (Aretxabaleta et al., 2008; Wang et al., 1994). Cyclonic gyres in shallow waters are expected to disperse the water, pollutants, and suspended matter, since anticyclonic gyres have been found to concentrate such substances (Salas-de-Leon et al., 2004a). Thus, it is important from an ecosystem standpoint to understand the physical mechanisms associated with such gyres in shallow systems and their relation to residence time of the water-borne substances, as well as their trajectories.

The description of gyres in estuaries has been based both on *in situ* data (Cloern et al., 1983; Geyer et al., 2000; Officer, 1981; Salas-Monreal and Valle-Levinson, 2009) and model outputs (Dalrymple et al., 1990; Spiteri et al., 2008). The Regional Oceanic Modeling System (ROMS), which is a free-surface, hydrostatic, primitive equation model has been successfully used to describe currents and channel dynamics in estuaries. Xinyu and Valle-Levinson (2007) performed numerical experiments to simulate river discharge, with and without the influence of tides, in a shallow estuary and to describe the buoyancy effects on the circulation. Using the ROMS, Scully et al. (2009) found that the dominant along-channel momentum balance in estuaries is not always between the pressure gradient and the bottom stress. The nonlinear advective acceleration term can be on the same order of magnitude. The ROMS has also been used to study lateral circulation and to estimate sediment transport in estuaries (Chen and Sanford, 2009). The suspension (or resuspension) and deposition of matter are processes of particular importance in estuarine systems and arise mainly due to the presence of cyclonic and anticyclonic gyres, respectively.

The goal of this study is to advance the understanding of flow patterns and gyres generated in shallow flat estuaries under the influence of winds, tides, and river discharges. A recent oil spill in Galveston Bay, Texas (USA) ($>635\ m^3$ on March 23, 2014), resulting from a barge and cargo ship collision in the Houston Ship Channel, provided the impetus for the present study (Houston Chronicle, April 6, 2014). Model simulations and comparison to *in situ* data were carried out for the month of April 2014 in Galveston Bay to elucidate the relative importance of the terms in the momentum equation and to describe the variability of tidally generated gyres under different wind forcing conditions. The Galveston Bay estuary represents an ideal set up for the present study since it includes two differently shaped sub-estuaries (Fig. 1) directly influenced by two rivers.

Galveston Bay, the second largest estuary in the Gulf of Mexico (Fig. 1), has a surface area of 1600 km^2, is 50 km long, and is 27 km wide. The bathymetry is relatively flat with a mean depth of 3 m, except in the northern entrance (Houston Ship Channel), where a 12 m deep channel is located (Dupuis and Anis, 2013). The bay has an intertidal range of 0.5 m. The bay is connected to the Gulf of Mexico *via* two inlets (southern entrance and northern entrance) and has two major freshwater sources, the San Jacinto and Trinity Rivers (Fig. 1). The estuary is one of the most important shipping hubs in the USA and home to the Port of Houston, the largest port in the USA, and based on foreign tonnage, this estuary is the sixth largest in the world. More than one-third of the USA chemical production facilities and oil refineries are located around the bay, and one-third of commercial fishing income and one-half of sport fishing expenditures in Texas come from the estuary. Previous studies have already described the general dynamics of the bay using model simulations to reproduce the general circulation (Rayson et al., 2015), the effect of hurricanes within the bay (Rego and Li, 2010), and the effect of varying fresh water inputs on the oyster population within Galveston Bay (Klinck et al., 2002).

This manuscript reports the results of a study that explores the dynamics of tidally formed cyclonic gyres in a shallow estuary. This manuscript incorporates field observations and model simulation results and addresses the following three main objectives: (1) the variability of tidally generated gyres under different wind forcing conditions, (2) the distance of the river influence on the estuary and (3) the relative importance of the terms in the momentum equation.

2. Material and methods

The ROMS has been used to model internal tides and to estimate tidal fields, mixing and current patterns (Robertson, 2006; Salas-de-Leon et al., 2004a; Scully et al., 2009; Sutherland et al., 2011; Xinyu and Valle-Levinson, 2007). According to Robertson (2006), the semidiurnal baroclinic tides are well simulated with ROMS. The free-surface, hydrostatic, primitive equation ocean model uses sigma coordinates in the vertical (Haidvogel et al., 2000) to increase the accuracy of the simulations. In this study, the ROMS was setup following the basic configuration described in Salas-Monreal et al. (2012) to elucidate the effect of the wind stress in a shallow estuary and the influence of fresh water inputs on flow dynamics. The model was configured for the domain shown in Fig. 1. At the locations of freshwater inflow into the estuary (San Jacinto and Trinity Rivers), salinity was assumed to be zero and temperature equal to 15°C. River velocity discharges were set to $0.40\ m\ s^{-1}$ for both rivers ($\sim 100\ m^3\ s^{-1}$), which are representative values for this time of the year according to O'Donnell (2005). Tidal sea surface elevations, used to force the model at the external boundary, were obtained from the North Jetty station located at the entrance of the Galveston Bay (Fig. 1; http://tidesandcurrents.noaa.gov/harcon.html?id=8771341). Initial ocean salinity and temperature (inside and outside of the

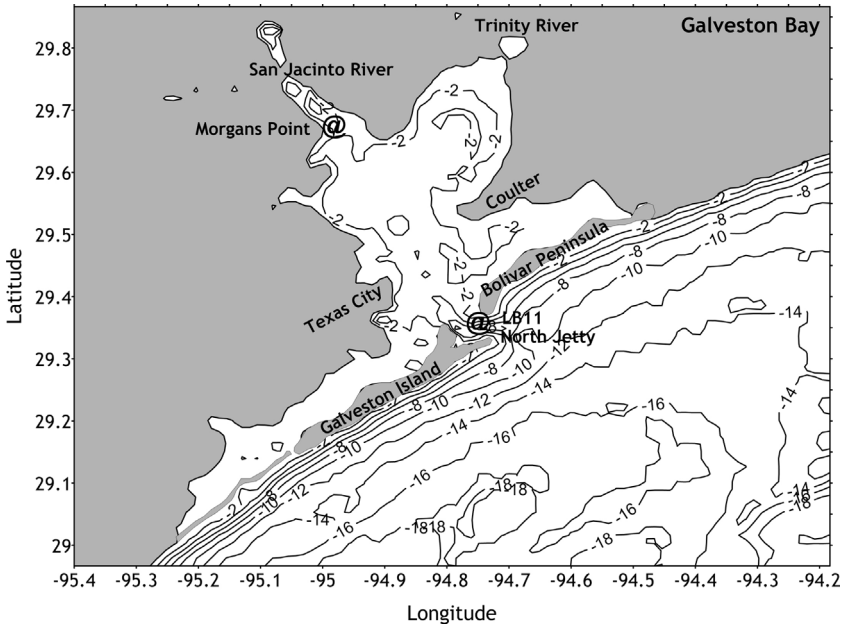

Figure 1 Galveston Bay and locations of the northern and southern entrances and the San Jacinto and Trinity Rivers. The @ symbols represent the location of the Morgans Point, LB11, and North Jetty tide stations. Two subestuaries are visible, one off the San Jacinto River with an elongated shape, and the second off the Trinity River with a roughly circular shape.

bay) were uniformly set throughout the entire domain to 22 and 34°C, respectively. The vertical eddy diffusivity uses a Mellor-Yamada closure scheme, as has typically been used in estuaries and bays (Fong, 1998).

The model domain has 64 × 84 grid points with 10 sigma coordinates. Using these sigma coordinates, the vertical resolution varies from <0.5 m in the flat part of the estuary to ~1 m at the channel (northern entrance). The resolution 64 × 84 grid points (~1.5 × 1 km of horizontal resolution) were chosen since gyres are often masked by insufficient grid resolution (Lynch et al., 1995). The free surface elevation, which uses the "Flather condition" (Marchesiello et al., 2001), the salinity, temperature, and water velocities at each grid point were recorded at 0.5 hourly intervals after the model had reached stability. Bottom stress was assumed to be a quadratic function of the bottom velocity with a drag coefficient of 2.5×10^{-3}. The tidally averaged potential and kinetic energy were calculated for each grid point. Once the normalized differences in energy from successive iterations were on the order of 10^{-3} or lower ($((E_{i+1}-E_i)/E_i \leq 0.001)$, the model was considered stable; this occurred after 28 simulation days.

A total of five experiments were conducted. The first experiment was conducted assuming a zero wind velocity to elucidate the circulation within the estuary resulting solely due to tidal forcing. The next four experiments were conducted assuming a constant wind speed of 10 m s^{-1} blowing from a southeastern, southwestern, northeastern and northwestern direction, respectively, to elucidate the residual flow under relatively strong and sustained wind conditions. These winds were chosen based on the conclusion of Park et al. (2001) that the winds that most significantly affect the estuary blow from the southeast with speeds of ~8 m s^{-1}. The wind speed in this study was set to 10 m s^{-1} based on observations of the seasonal wind velocities observed from the simulation period in the estuary, as reported by the National Weather Service (http://www.srh.noaa.gov/hgx/).

2.1. Initial model simulations and calibration

Tidal components and phases were obtained at four NOAA stations (Table 1) to classify the tides within the estuary. Based on the tide information from these stations, the form factor (F = (K1 + O1)/(M2 + S2)) (Salas Pérez et al., 2012) classifies the estuary itself as diurnal ($F > 3$), while at the entrance of the estuary, tides are classified as mixed, mainly diurnal ($1.5 < F < 3$). To obtain residual flows from *in situ* observations, it is thus necessary to perform at least six measurements per day (Nyquist frequency = 3 cyc day^{-1}) to reproduce a semidiurnal sinusoidal signal. At least twelve measurements will allow for the reproduction of the inflexion points of a tidally mixed (mainly diurnal) signal (Chacon-Gomez et al., 2013), as well as for the obtaining of subtidal flows from *in situ* data within the estuary.

The model was forced at the external ocean boundary with tidal components and phases calculated from the sea-level observations at the North Jetty station (Fig. 1). Here, only the seven largest tidal amplitudes (Table 2) were used, as they could accurately reproduce the observed tidal signal at the North Jetty station (Fig. 2; correlation of 0.82 and a p-value < 0.05, which imply the matching of phase). These tidal components were calculated using a two-year time series at the North Jetty station.

Tidal simulations, recorded hourly, were compared to measured sea surface elevations obtained from the North Jetty and Morgans Point stations, as seen in Fig. 2. A higher correlation (0.82) was present between the simulated sea level and the observed time series at the North Jetty station than between the simulated harmonics and the Morgans Point station time series (0.73). This finding maybe attributed to river discharges from the San Jacinto River (causing the sea elevation to rise), to the amplification/attenuation of the diurnal/semidiurnal tides due to the relative shallowness of the bay or simply as a result of using the North Jetty tides to

Table 1 Amplitudes, form factor (F = (K1 + O1)/(M2 + S2)), and classification for the four main tide constituents at the four NOAA stations in Galveston Bay.

Station	Latitude	Longitude	K1 (m)	O1 (m)	M2 (m)	S2 (m)	F	Tide classification
North Jetty	29°21.4′N	94°43.5′W	0.466	0.420	0.381	0.095	1.86	Mixed, mainly diurnal
Port Bolivar	29°21.5′N	94°47.5′W	0.464	0.459	0.260	0.080	2.71	Mixed, mainly diurnal
Eagle Point	29°28.9′N	94°55.0′W	0.384	0.374	0.113	0.038	5.02	Diurnal
Morgans Point	29°40.9′N	94°59.1′W	0.473	0.454	0.208	0.053	3.55	Diurnal

Table 2 The seven major tide constituents (North Jetty tide station) used to force the model at the external ocean boundary.

Constituent	Amplitude (m)	Phase	Speed (m s^{-1})
M2	0.381	108.1	28.984
S2	0.095	117.5	30.000
N2	0.105	87.0	28.439
K1	0.466	307.0	15.041
O1	0.420	313.2	13.943
SSA	0.282	55.1	0.082
SA	0.217	155.4	0.041

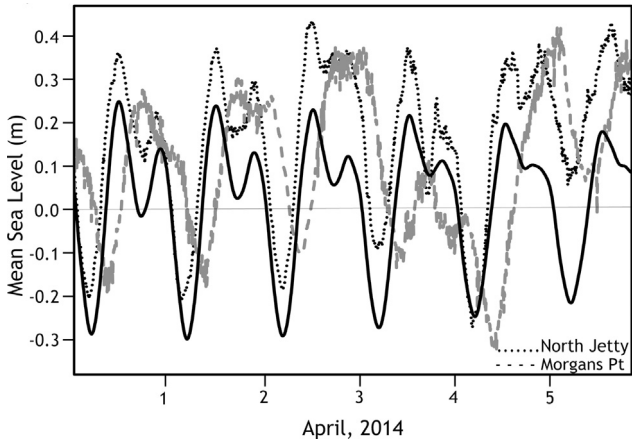

Figure 2 Time series of observed hourly mean sea level (m) at the North Jetty (dotted lines), Morgans Point (dashed lines) and the simulated sea level (solid line).

force the model (http://www.srh.noaa.gov/hgx). In addition, a time lag of 0.42 h was observed between the two stations.

Since the ROMS (3D model) is a hydrostatic model, two conditions were tested, the first condition being (Ro) $(alpha)^2 \ll 1$ and the second condition being (Fr)^2 $(alpha)^2 \ll 1$. Here, $alpha = H\,L^{-1}$ is the aspect ratio of the motion, Ro is the Rossby number (U/fL) and Fr is the Froude number (U/NH), in which U is the velocity scale, L and H are the length and depth scale, respectively, f is the Coriolis parameter, and N is the Brunt–Vaisala frequency. Finally, the Ekman layer thickness $(2k/f)^{1/2}$ (where k is the eddy viscosity scale) is approximately 4.5 m, and since the depth of the bay is ~3 m, its dynamics could be considered frictional (surface and bottom). As shown in Fig. 3, the model could reproduce the temperature time series at both stations ($r^2 > 0.79$ and a

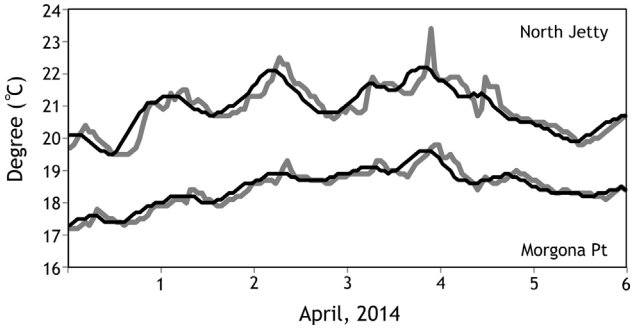

Figure 3 Time series of observed surface temperature (°C) at North Jetty, and Morgans Point (gray) and simulated surface temperature (solid black line) at the same locations.

p-value < 0.05). However, a time lag was noted between the observed and simulated temperatures, which was attributed to an increase in cold river inflow of fresher water to the estuary, as a result of several rain events during this period. The lag would thus not be simulated by the model since constant values were used for river water discharge, salinity, and temperature. Once the model was validated, the outputs were used to describe the temperature, salinity and current fields throughout the bay.

3. Results and discussion

3.1. Model simulations with no wind conditions

Once the model was calibrated, five experiments were performed. The first experiment was performed assuming no winds to describe the tidal effects on sea surface temperature (SST), salinity and current fields (1 m depth). The simulated temperature field for April 4th, 2014, exhibits a surface gradient of up to 4°C between the northern entrance and San Jacinto River during ebb (Fig. 4b) and up to 3°C during flood (Fig. 4a). The difference in SST gradient of ~1°C, observed between ebb and flood tides, was also evident up to a distance offshore corresponding to the 14 m depth isobaths or 10 km offshore (Isotherms of ~22.5°C). The simulations suggest that this is roughly the offshore distance of influence of the discharges of the San Jacinto and Trinity Rivers and thus likely the offshore distance where estuarine-borne matter might be directly affected by the diurnal tidal cycle. This can be corroborated by satellite images which show a color gradient (sediment gradient) at this location. The simulated residual temperature (Fig. 4c), obtained after filtering the diurnal tidal signal, suggests that the temperature in the estuary was modified at both bay entrances

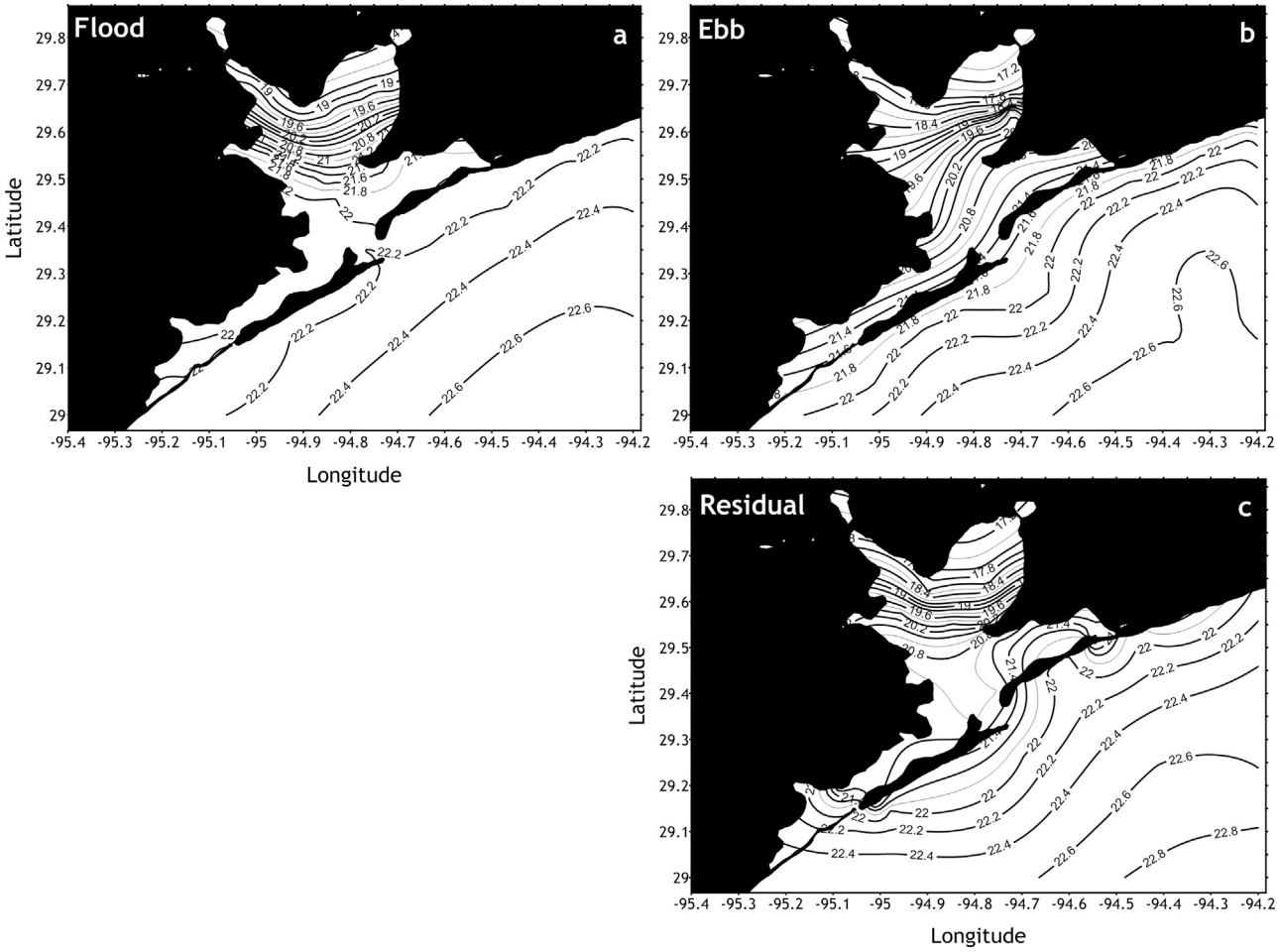

Figure 4 Surface temperature fields (contour lines are at 0.2°C intervals) obtained from model simulations during flood (a), ebb (b), and the residual (c) for April 4th, 2014.

(Fig. 1). The southern entrance exhibited a higher spatial temperature gradient ($\sim 4.0 \times 10^{-5}$°C m^{-1}) than that observed at the northern entrance ($\sim 1.1 \times 10^{-5}$°C m^{-1}). This finding may appear opposite to what one may expect, since the northern entrance shows a higher influence by the river discharge (*e.g.*, lower temperatures) compared to the southern entrance. However, lower mixing rates, associated with the lower volume transport at the southern entrance compared to that observed at the northern entrance, may provide a plausible explanation for the difference in the temperature gradients. Inside the estuary, a stronger temperature gradient was observed at a latitude near the Coulter "tongue" (29.55°N, Fig. 1). At this latitude, the discharges of the San Jacinto and Trinity Rivers have the largest influence within the estuary. This area is expected to be one with relatively higher concentrations of organisms, due to nutrient transport by the rivers, and organic pollutants originating from the Houston metropolitan area. This was also confirmed by Chlorophyll-*a* satellite images (Zhang et al., 2014).

Surface salinity differences between the entrances and the river mouths during flood (Fig. 5a) and ebb (Fig. 5b) tides had a vertical salinity gradient of $\sim 27 \times 10^{-5}$ and $\sim 21 \times 10^{-5}$, respectively. Lower salinities were found near the Trinity River (14) and higher salinities were observed near the southern entrance of the bay (>26). The higher salinities observed at the southern entrance may be attributed to a combined influence of the open ocean and the larger distance from the San Jacinto and Trinity Rivers compared to that of the northern entrance. Although planktonic organisms can be biologically active at times (for which the present simulations do not account), there are similarities between the diffusion and advection of salt and plankton (Valle-Levinson et al., 2004). In such cases, it may be assumed that plankton will move in and out of the estuary following patterns similar to those of salinity. Thus, it seems reasonable to expect that in the present scenario, plankton will move out and into the estuary at a latitude near Coulter (Fig. 1).

The influence of the rivers, based on salinity values obtained from model simulations, was observed seaward to a distance where the 14 m depth isobath is located or ~10 km offshore (isohaline of ~32). This is also the distance where satellite images show a color gradient (sediment gradient). Thus, based on the hydrographic properties from the simulations, it is suggested that the influence of the rivers may be observed to a distance offshore of ~10 km, commensurate with the 14 m depth isobath. This is also the distance offshore that water-borne matter from the estuary may reach during a tidal cycle under calm (no winds) conditions. The simulated residual surface salinity exhibits a difference of 12 between the entrance and the river mouth (Fig. 5c).

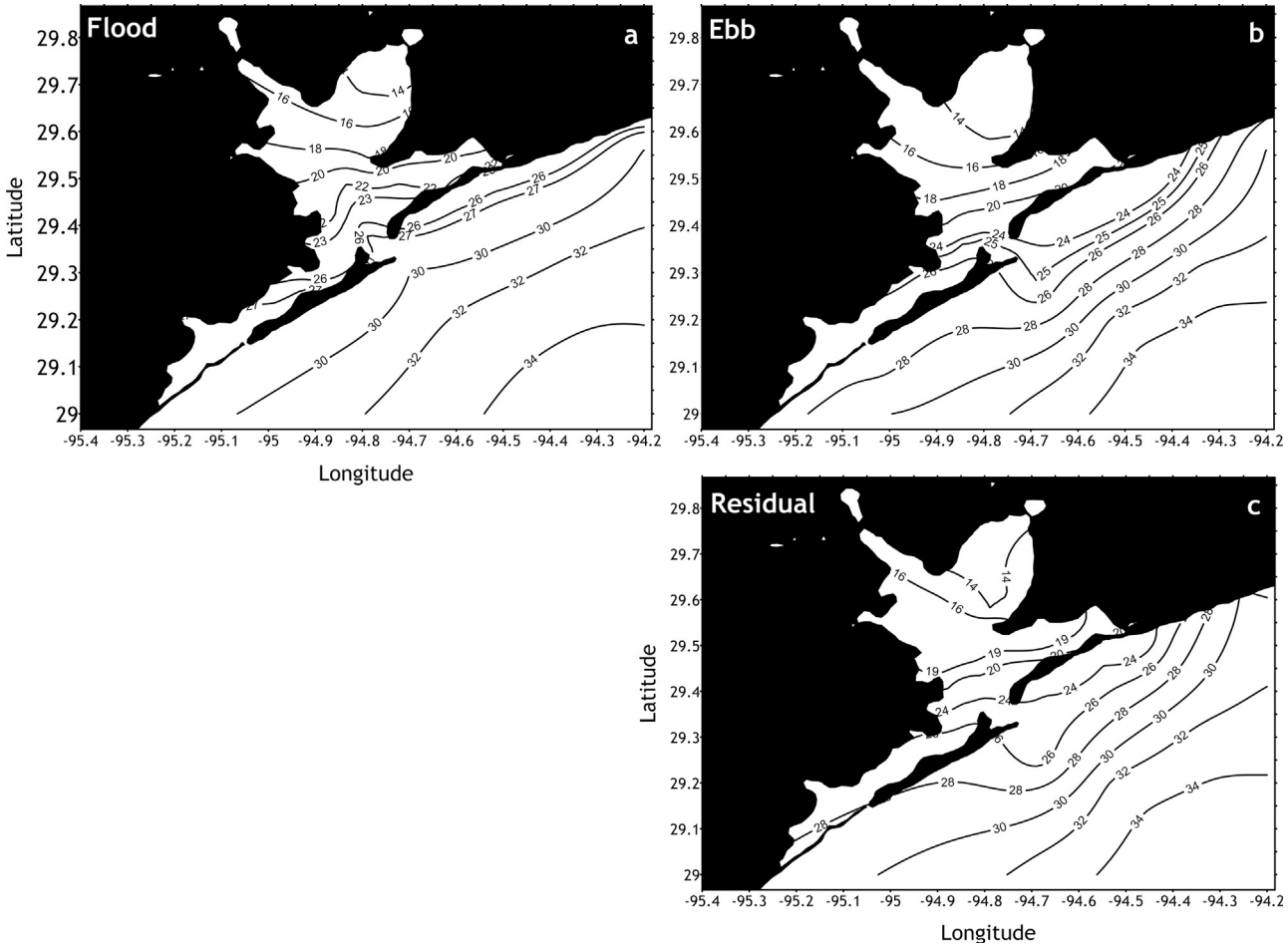

Figure 5 Surface salinity fields (contour lines are at 2 intervals) obtained from model simulations during flood (a), ebb (b) and the residual (c) for April 4th, 2014.

An interesting feature is an increase in salinity from 14 to 16 near Trinity River toward Coulter (a horizontal gradient of 6×10^{-5}). This feature appears to be attributed to a cyclonic gyre and is supported here by the pattern of the residual velocity currents shown in Fig. 6c. High productivity areas have been associated with cyclonic gyres through the pumping of nutrient-rich deep water in coastal areas (Salas Pérez et al., 2012; Salas-de-Leon et al., 2004b; Salas-Monreal et al., 2009). In the case of Galveston Bay, a cyclonic gyre is expected to be highly productive since the current trajectories confine river discharges from the San Jacinto and Trinity Rivers into this area. Such a confluence of currents may also concentrate a variety of water-borne substances and suspended particles, including oil derivatives and pollutants, as is suggested by the satellite images (high dark color or sediments in this area).

During flood tides the gyre appears to be displaced northward toward the Trinity River mouth, while during ebb, it is displaced southward toward the Coulter "tongue" (Fig. 6a, b). In contrast, the San Jacinto River area exhibits a bidirectional flow, with inflow during flood and outflow during ebb. The difference in current fields might be attributed to the shapes of these bays; while the San Jacinto subestuary has an elongated shape, the Trinity subestuary has a circular shape that allows the cyclonic gyre to develop during a tidal cycle. In general, water velocity simulations never reached speeds above 0.7 m s^{-1}. These values are consistent with the flow velocity previously reported by Klinck et al. (2002) and reported by the Gulf of Mexico Foundation (http://www.gulfmex.org/).

The residence time of the estuary, calculated using the velocity simulations, was estimated to be ~18.5 h. Velocities were also used to calculate volume fluxes at the estuary entrances. Most of the water was found to exit the estuary through the northern entrance (55,200 m^3 s^{-1}) while only 18% exits through the southern entrance (12,400 m^3 s^{-1}). However, due to the gyre and the shape of the coastline, it is expected that areas with residence times larger than 18.5 h may exist, such as in the northern part of the bay (Rayson et al., 2015) or at the gyre location. These regions are expected to be locations with high biological productivity and high concentrations of water-borne substances such as pollutants and suspended particles.

The cyclonic gyre is not expected to generate a highly productive area through the commonly observed pumping mechanism of deep nutrient-enriched waters due to the shallowness of the subestuary (~3 m depth; Fig. 1). However, the gyre may introduce nutrients through resuspension of the bottom sediments and/or by concentrating higher nutrient content waters from the rivers into the subestuary. This

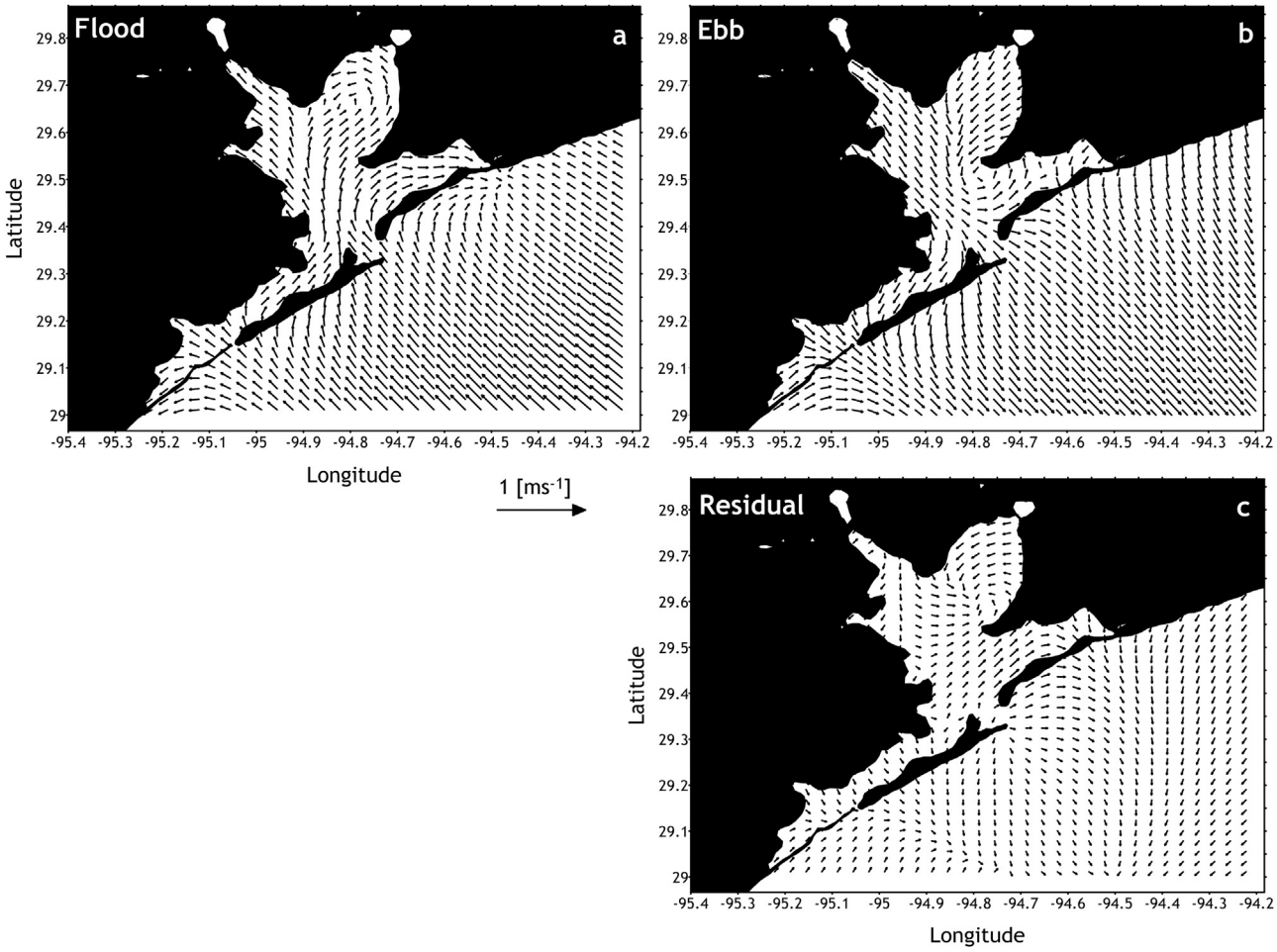

Figure 6 Surface velocity fields (m s^{-1}) obtained from model simulations during flood (a), ebb (b) and the residual (c) for April 4th, 2014.

finding was also suggested by means of satellite images (Zhang et al., 2014).

3.2. Two-layer flow

Even though Galveston Bay is a shallow and relatively flat micro-tidal estuary, the flow at the northern entrance forms a two-layer system (Fig. 7) and is influenced by the Coriolis acceleration, as can be observed from the upward tilt at the northern end of the bottom-layer inflow (Fig. 7c, right side). Bottom friction plays an important role since the core of the inflow (0.5 m s^{-1}) is located at a depth of 6 m, which is about three-quarters of the overall water depth at the estuary northern entrance. The strongest outflows were observed near the surface at the southern end of the northern entrance due to the Coriolis acceleration. The maximum cross-channel flow speed (Fig. 7b) at the northern entrance was ~0.2 m s^{-1}, which is less than 30% of the along-channel flow speed (Fig. 7a; ~0.5 m s^{-1}). When flow scales in an estuary are much larger than the Rossby radius of deformation, the circulation within the estuary can be considered in geostrophic balance. The Rossby radius of deformation (Gill, 1982) for Galveston Bay is $\sim 1.4 \times 10^5$ m, while the estuary scale is $< 1 \times 10^5$ m. Thus, it is expected that friction will play a significant role in the momentum balance. Here, the influence of the Coriolis acceleration term appears to be evident in the two-layer residual flow structure from the upward tilt of the bottom flow at the right side of the channel (~30°N), while the influence of friction is evident from the vertical location of the core of the inflow.

The model does not account directly for zooplankton concentrations since it does not contain an ecosystem model. However, it is commonly noted that in estuaries with irregular bathymetry, planktonic organisms concentrate close to the pycnocline depth (Lennert-Cody and Franks, 1999; Ryan et al., 2005; Shanks, 1983; Zeldis and Jillett, 1982). In this case, a large fraction of organisms will be located at a depth of ~5 m at the entrance of the estuary. Nevertheless, zooplankton has been observed to cross the pycnocline depending on the hour of the day and the state of turbulence levels in the water (Heywood, 1996).

Since the flow exchange through the northern entrance is approximately 4 times that through the southern entrance, it is expected that most of the estuarine-ocean exchange of water-borne constituents will occur through the northern entrance. In addition, since the tides are mainly diurnal (Table 1), it may be expected that organisms (*e.g.*, plankton) will enter and exit the estuary once a day following the diurnal tidal cycle.

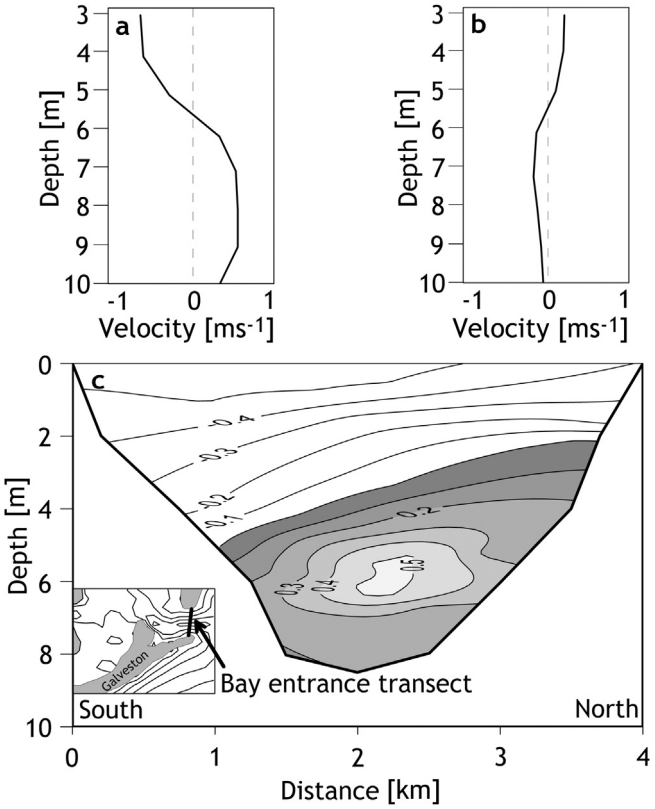

Figure 7 Simulated residual velocities at the northern entrance. (a) Along-channel; (b) cross-channel; (c) along-channel flow through a cross channel transect. Positive values indicate inflow, while negative values indicate outflow, for April 4th, 2014.

During a diurnal tidal cycle, the bulk of oceanic organisms is expected to be concentrated near the northern end of each of the two entrances, while estuarine organisms may concentrate near the southern ends of the entrances due to the Coriolis acceleration. Fig. 8 represents simulations of Lagrangian surface drifters/particles released at the southern part of the model domain (Fig. 8a) and at both estuary entrances (Fig. 8b). The drifters/particles were released at each grid point of the border domain (84 points) and at the bay entrances (8 points); however, due to the number of points, only 10 drifters/particles are shown in Fig. 8a and only 3 drifters/particles are shown in Fig. 8b. Simulations suggest that more than 60% of the drifters/particles released at a distance of up to 30 km from the northern entrance (Fig. 8a) will enter and leave the estuary during a single diurnal tidal cycle. Therefore, even though the river influence was observed to a distance of ∼10 km seaward from the mouth of the estuary, most of the water-borne constituents located at a distance of ∼30 km may be expected to enter and exit the estuary during a diurnal tidal cycle. This is of particular importance to our understanding of the ecosystem of Galveston Bay, since the estuarine-ocean exchange of nutrients, planktonic organisms, and other water-borne biota is likely to follow patterns similar to those of the Lagrangian drifters. Furthermore, Fig. 8b shows that even though the particles released at the northern entrance were very close to each other, they have two different paths, showing that the trajectories are quite sensitive to the initial position of the particles.

3.3. Model simulations under seasonal wind conditions

Since Galveston Bay is a shallow micro-tidal system, winds (surface stress) are expected to play an important role in the local dynamics. To examine this further, four experiments were performed by forcing the model with tides and constant winds of 10 m s^{-1} blowing from four different directions: southeasterly (SE; Fig. 9a), southwesterly (SW; Fig. 9b), northeasterly (NE; Fig. 9c) and northwesterly (NW; Fig. 9c). All the experiments showed differences between one another; however, in all cases, the tidally formed gyre diminished in strength, or even disappeared, under these winds conditions. Under SE and SW wind-stress forcing, the cyclonic gyre (positive vorticity) was observed in the Trinity subestuary (Fig. 9a, b) but diminished in strength with the vorticity reduced by $\sim 1 \times 10^{-4}$ s^{-1}, compared to the vorticity value obtained under no wind conditions ($\sim 3 \times 10^{-4}$ s^{-1}). Due to the wind direction (for both SW and SE), water piled up at the estuary region located between the Coulter "tongue" and the Bolivar Peninsula forming a pressure gradient, $((1/\rho)(\partial P/\partial y))$, larger than 0.9×10^{-5} m s^{-2}, along the subestuary. This is significantly higher than the pressure gradient (0.2×10^{-5} m s^{-2}) observed when the model was forced solely by tides. Under NE and NW wind-stress forcing (Fig. 9c, d), the cyclonic gyre formation was not observed. However, during NW winds, water piled up at the region located between the Coulter "tongue" and the Bolivar

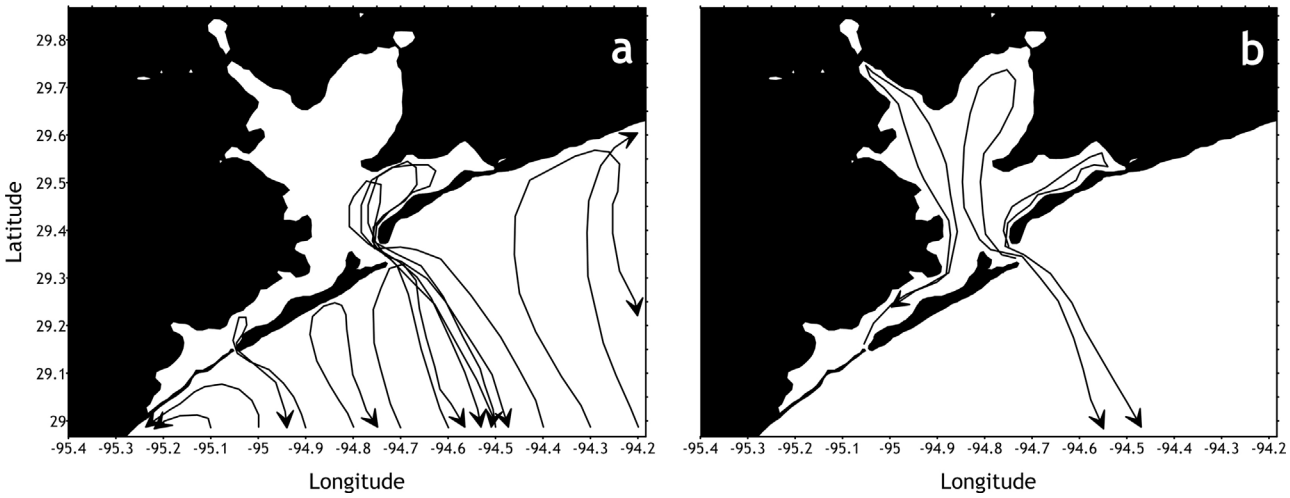

Figure 8 Simulations of Lagrangian surface drifters/particles. (a) Paths of drifters released at intervals of 0.1° longitude, starting at the southern edge of the domain, during one diurnal cycle; (b) three Lagrangian surface drifters/particles followed during one diurnal tidal cycle. Two drifters were released at the northern entrance and one at the southern entrance to the bay. Filled arrow heads represent the location of the drifters at the end of the diurnal tidal cycle for April 4th, 2014.

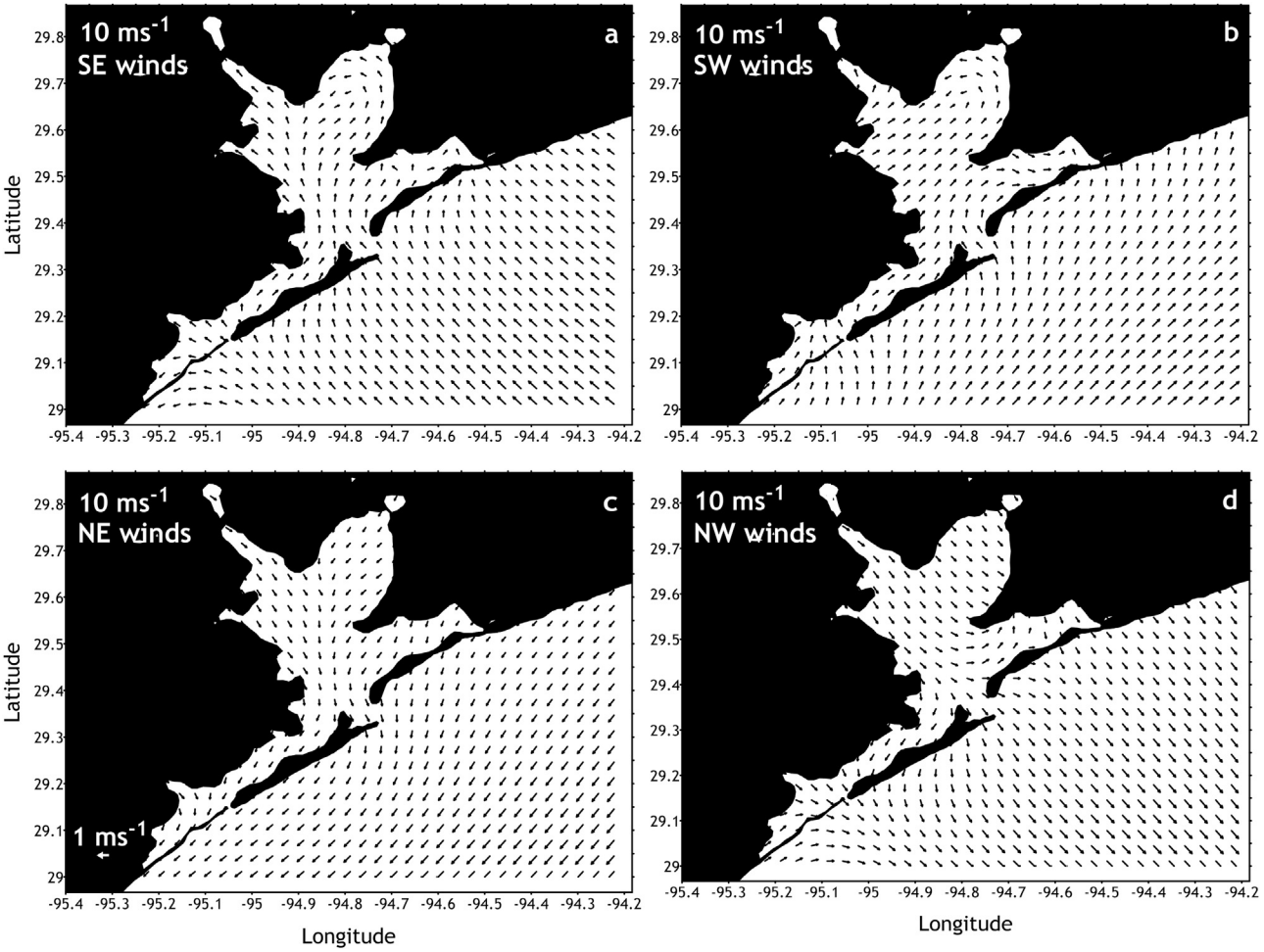

Figure 9 Residual velocity fields (m s^{-1}) obtained from model simulations under sustained southeasterly (a), southwesterly (b), northeasterly (c), and northwesterly (d) wind conditions. Wind speed for all cases was set to 10 m s^{-1}.

Peninsula. This pile-up appears to be associated with the current trajectories advecting water from the San Jacinto River to this region (Fig. 9d). The pressure gradient formed along the estuary was found to be weaker (0.7×10^{-5} m s^{-2}) than that under either SE or SW wind conditions. Under NE wind conditions, the entire estuary could flush, providing a means for water-borne substances, pollutants, and planktonic organisms to exit the estuary through both entrances. The NE winds constituted the only wind forcing conditions allowing the entire bay to flush. Due to the geometry of the San Jacinto subestuary (elongated shape), only NE and NW winds could flush it, while the Trinity subestuary (circular shape) was observed to fully flush only under NE winds. Southeasterly winds, with speeds of ~8 m s^{-1}, are the most common winds in Galveston Bay (Park et al., 2001). Thus, the observed cyclonic gyre is likely to be present most of the time, possibly creating a region with elevated concentrations of suspended particles and planktonic organisms. Under NE and SE wind conditions, the influence of the rivers was observed up to 6 km offshore, while under SW and NW wind conditions, the influence of the rivers was observed up to 12 km; therefore, the SW wind conditions create the farthest influence of the river offshore. Using the National Weather Service data at Galveston, it could be inferred that from October to April, the dominant southerly winds will not allow the entire bay to flush out, while from May to September, the dominant northerly winds may favor flushing of the entire bay.

3.4. Scale analysis

To describe the dynamics at Galveston Bay, a scale analysis of the momentum equation (Eq. (1)) was performed following (Emery and Thomson, 2001).

$$\frac{\partial V}{\partial t} + u\frac{\partial V}{\partial x} + v\frac{\partial V}{\partial y} + W\frac{\partial V}{\partial z} + fu = \frac{1}{\rho}\frac{\partial P}{\partial y} + \frac{\partial}{\partial z}\left(k\frac{\partial V}{\partial z}\right). \quad (1)$$

In Eq. (1), t is time; u, v, and w are velocity components in the x (east), y (north) and z (down) directions, respectively; f is the Coriolis parameter; ρ is seawater density; P is total pressure; and k is the vertical eddy viscosity. Eq. (1) presents the tidal current plus the residual current; therefore, an average process of 25 h was applied to remove the tidal stresses (advection terms of tidal current) in the momentum equation. The magnitude of the terms in the momentum Eq. (1) for the residual flow were computed by vertically and horizontally averaging over the elongated and circular estuary and resulted in the following values: [0.6 + 1.1 + 0.6 + 0.3 + 0.1 = 1.2 + 1.5] $\times 10^{-5}$ m s^{-2} for the elongated estuary and [0.4 + 0.8 + 1.2 + 0.1 + 0.2 = 0.8 + 1.9] $\times 10^{-5}$ m s^{-2} for the circular estuary. Friction along the surface and bottom had a more pronounced effect in shallow waters because friction can affect the entire water column (<3 m on average for Galveston Bay), whereas advection had a larger effect near the river mouths (Fig. 10). Thus, the local dynamics appear to be governed mainly by friction, due to the shallowness of the bay, and advection, due to the river discharges. However, once the wind relaxes, the pressure gradient terms, $\partial P/\partial y$ and $\partial P/\partial x$, become important in the local dynamics due to water piling up in the region between the Coulter "tongue" and the Bolivar Peninsula. Therefore, the dynamics of both subestuaries were the same regardless of the subestuary shape and the distance to the Galveston Bay mouth. Finally, at the northern entrance, Coriolis acceleration appears to play an important role in the local dynamics. As noted above, this can be clearly observed from the intensification and upward tilt of both the inflow and outflow at the northern side of the entrance (Fig. 7c, right side) and as further confirmed by the scale analysis.

4. Conclusions

Model outputs and *in situ* data from Galveston Bay, Texas (USA), a shallow, relatively flat estuary with two subestuaries, one elongated and one roughly circular, were used to elucidate the wind-stress effects on a tidally formed cyclonic gyre in the circular subestuary. Tidal amplitudes were used to calculate the form factor, which suggested that the estuary is a diurnal system with tides that have a phase difference of less than 1 h within the estuary. The simulated hydrographic data (temperature and salinity) showed that the river influence can be observed up to a distance commensurate with the 14 m depth isobath (~10 km offshore) during a diurnal

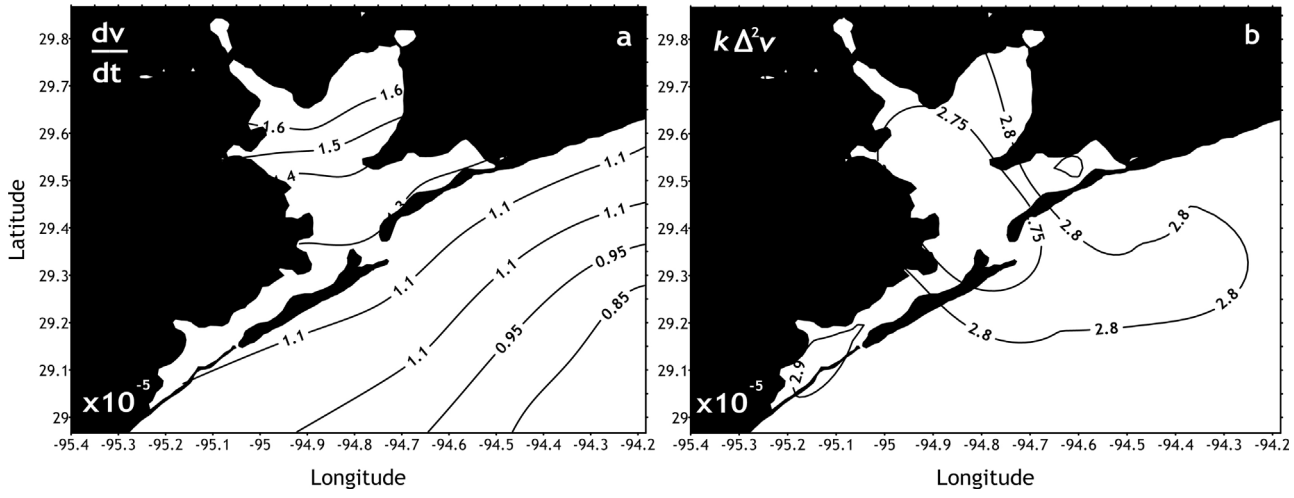

Figure 10 Residual acceleration terms: (a) advection (dv/dt) and (b) friction under southeasterly wind conditions ($k\Delta^2 v$).

tidal cycle and up to 12 km offshore under SW wind conditions. However, the most significant influence of the main rivers (San Jacinto and Trinity) was observed in the region where the two subestuaries meet (at the Coulter Peninsula latitude), which is also the region where the cyclonic gyre was observed.

The tidally formed gyre appeared to be further enhanced through the combined effect of the circular shape of the subestuary and the confluence of the river outflow. The current trajectories of the gyre confine the river discharges from the San Jacinto and Trinity Rivers into this area as well. Thus, it is expected that elevated concentrations of nutrients may be found in this area, resulting in higher productivity rates than elsewhere in the bay, as described in previous studies with chlorophyll-*a* data (Zhang et al., 2014). Adding wind forcing to the simulations showed a general weakening of the gyre when winds were applied from various directions. In particular, the gyre was observed to disappear under northerly wind conditions.

More than 82% of the inflow-outflow transport was observed to occur through the northern entrance of the estuary while less than 18% occurred through the southern entrance. The residence time of the bay, calculated using the water velocity simulations, was found to be less than 18.5 h. However, due to the tidally formed cyclonic gyre and the shape of the coast line, water may reside for a longer period of time in the area influenced by the gyre. Rayson et al. (2015) described the residence time in the upper bay area to be up to 50 days. The estuary was found to flush completely only under the forcing of northeasterly winds, mostly from October to April. These were also the wind conditions under which the gyre was observed to disappear completely.

Based on a scale analysis of the momentum equation, friction (at the surface and the bottom) and advection were found to be the dominant terms in the estuary. However, the pressure gradient and Coriolis acceleration terms were found to be particularly significant near the northern entrance to Galveston Bay.

Acknowledgements

This project was supported by a sabbatical grant from CONACYT number 232872. We also acknowledge the National Oceanic and Atmospheric Administration (NOAA) for data availability.

Appendix A. Supplementary data

Supplementary data associated with this article can be found, in the online version, at doi:10.1016/j.oceano.2017.10.005.

References

Agardy, T., 2000. Effects of fisheries on marine ecosystems: a conservationist's perspective. ICES J. Mar. Sci. 57 (3), 761—765, http://dx.doi.org/10.1006/jmsc.2000.0721.

Aretxabaleta, A.L., McGillicuddy, D.J., Smith, K.W., Lynch, D.R., 2008. Model simulations of the Bay of Fundy Gyre: 1. Climatological results. J. Geophys. Res. Oceans 113 (C10), C10027, http://dx.doi.org/10.1029/2007JC004480.

Avendaño-Alvarez, O., Salas-Monreal, D., Marin-Hernandez, M., Salas-de-Leon, D.A., Monreal-Gomez, M.A., 2017. Annual hydrological variation and hypoxic zone in a tropical coral reef system. Reg. Stud. Mar. Sci. 9, 145—155, http://dx.doi.org/10.1016/j.rsma.2016.12.007.

Becerro, M.A., Bonito, V., Paul, J.V., 2006. Effects of monsoon-driven wave action on coral reefs of Guam and implications for coral recruitment. Coral Reefs 25 (2), 193—199, http://dx.doi.org/10.1007/s00338-005-0080-7.

Chacon-Gomez, I.C., Salas-Monreal, D., Riveron-Enzastiga, M.L., 2013. Current pattern and coral larval dispersion in a tropical coral reef system. Cont. Shelf Res. 68, 23—32, http://dx.doi.org/10.1016/j.csr.2013.08.014.

Chen, S.N., Sanford, L.P., 2009. Lateral circulation driven by boundary mixing and the associated transport of sediments in idealized partially mixed estuaries. Cont. Shelf Res. 29 (1), 101—118, http://dx.doi.org/10.1016/j.csr.2008.01.001.

Cloern, J.E., Alpine, A.E., Cole, B.E., Wong, R.L., Arthur, J.F., Ball, M.D., 1983. River discharge controls phytoplankton dynamics in the northern San Francisco Bay estuary. Estuar. Coast. Shelf Sci. 16 (4), 415—429, http://dx.doi.org/10.1016/0272-7714(83)90103-8.

Dalrymple, R.W., Knight, R., Zaitlin, B.A., Middleton, G.V., 1990. Dynamics and facies model of a macrotidal sand-bar complex, Cobequid Bay—Salmon River Estuary (Bay of Fundy). Sedimentology 37 (4), 577—612, http://dx.doi.org/10.1111/j.1365-3091.1990.tb00624.x.

Dupuis, K.W., Anis, A., 2013. Observations and modeling of wind waves in a Shallow Estuary: Galveston Bay, Texas. J. Waterw. Port C-ASCE 139 (4), 314—325, http://dx.doi.org/10.1061/(ASCE)WW.1943-5460.0000160.

Emery, W.J., Thomson, R.E., 2001. Data Analysis Methods in Physical Oceanography. Elsevier Sci., New York, 638 pp.

Fong, D.A., 1998. Dynamics of freshwater plumes: observations and numerical modeling of the wind-forced response and alongshore freshwater transport. (Ph.d. thesis). Massachusetts Institute of Technology and Woods Hole Oceanographic Institution, http://dx.doi.org/10.1575/1912/4784.

Geyer, W.R., Trowbridge, J.H., Bowen, M.M., 2000. The dynamics of a partially mixed estuary. J. Phys. Oceanogr. 30 (8), 2035—2048, http://dx.doi.org/10.1175/1520-0485(2000)030<2035:TDOAPM>2.0.CO;2.

Gill, A.E., 1982. Atmosphere-Ocean Dynamics. Acad. Press, Orlando, 662 pp.

Goreau, T.J., Hayes, R.L., 1994. Coral bleaching and ocean "hot spots". Ambio 23, 176—180.

Haidvogel, D.B., Arango, H.G., Hedstrom, K., Beckmann, A., Malanotte-Rizzoli, P., Shchepetkin, A.F., 2000. Model evaluation experiments in the North Atlantic Basin: simulations in nonlinear terrain-following coordinates. Dyn. Atmos. Oceans 32 (3—4), 239—281, http://dx.doi.org/10.1016/S0377-0265(00)00049-X.

Heywood, K.J., 1996. Diel vertical migration of zooplankton in the Northeast Atlantic. J. Plankton Res. 18 (2), 163—184, http://dx.doi.org/10.1093/plankt/18.2.163.

Holliday, D.V., Pieper, R.E., 1980. Volume scattering strengths and zooplankton distributions at acoustic frequencies between 0.5 and 3 MHz. J. Acoust. Soc. Am. 67 (1), 135—146, http://dx.doi.org/10.1121/1.384472.

Houston Chronicle, April 6, 2014. Oil spills in Galveston Bay a routine occurrence, http://www.houstonchronicle.com/news/science-environment/article/Oil-spills-in-Galveston-Bay-a-routine-occurrence-5381283.php.

Klinck, J.M., Hofmann, E.E., Powell, E.N., Dekshenieks, M.M., 2002. Impact of channelization on oyster production: a hydrodynamic-oyster population model for Galveston Bay, Texas. Environ. Model. Assess. 7 (4), 273—289.

Lennert-Cody, C.E., Franks, P.J., 1999. Plankton patchiness in high-frequency internal waves. Mar. Ecol.-Prog. Ser. 186, 59—66.

Lynch, D.R., Justin, T.C.I.P., Naimie, C.E., Werner, F.E., 1995. Convergence studies of tidally-rectified circulation on Georges bank. In: Lynch, D.R., Davies, A.M. (Eds.), Quantitative Skill Assessment for Coastal Ocean Models. AGU, 153—174.

Marchesiello, P., McWilliams, J.C., Shchepetkin, A., 2001. Open boundary conditions for long-term integration of regional oceanic models. Ocean Model. 3, 1—20, http://dx.doi.org/10.1016/S1463-5003(00)00013-5.

O'Donnell, H.W., 2005. Investigation of flood induced pipeline failures on lower San Jacinto River. In: Pipelines 2005. Optimizing Pipeline Design, Operations, and Maintenance in Today's Economy. 451—463, http://dx.doi.org/10.1061/40800(180)35.

Officer, C.B., 1981. Physical dynamics of estuarine suspended sediments. Mar. Geol. 40 (1—2), 1—14, http://dx.doi.org/10.1016/0025-3227(81)90039-6.

Park, J.S., Wade, T.L., Sweet, S., 2001. Atmospheric distribution of polycyclic aromatic hydrocarbons and deposition to Galveston Bay, Texas, USA. Atmos. Environ. 35 (19), 3241—3249, http://dx.doi.org/10.1016/S1352-2310(01)00080-2.

Rayson, M.D., Gross, E.S., Fringer, O.B., 2015. Modeling the tidal and sub-tidal hydrodynamics in a shallow, micro-tidal estuary. Ocean Model. 89, 29—44, http://dx.doi.org/10.1016/j.ocemod.2015.02.002.

Rego, J., Li, C., 2010. Storm surge propagation in Galveston Bay during Hurricane Ike. J. Mar. Syst. 82 (4), 265—279, http://dx.doi.org/10.1016/j.jmarsys.2010.06.001.

Robertson, R., 2006. Modeling internal tides over Fieberling Guyot: resolution, parameterization, performance. Ocean Dyn. 56 (5—6), 430—444.

Ryan, J.P., Chavez, F.P., Bellingham, J.G., 2005. Physical—biological coupling in Monterey Bay, California: topographic influences on phytoplankton ecology. Mar. Ecol.-Prog. Ser. 287, 23—32.

Salas Pérez, J.J., Salas-Monreal, D., Monreal-Gómez, M.A., Riveron-Enzastiga, M.L., Llasat, C., 2012. Seasonal absolute acoustic intensity, atmospheric forcing and currents in a tropical coral reef system. Estuar. Coast. Shelf Sci. 100, 102—112, http://dx.doi.org/10.1016/j.ecss.2012.01.002.

Salas-de-Leon, D.A., Diaz-Flores, M.A., Monreal-Gómez, M.A., 2004a. Circulation and vorticity in the Southern Gulf of Mexico. In: Schroeder, W. (Ed.), Hans Ertel Memorial Book, German Commission of History of Geophysics and Cosmical Physics. p. 229.

Salas-de-Leon, D.A., Monreal-Gomez, M.A., Signoret, M., Aldeco, J., 2004b. Anticyclonic-cyclonic eddies and their impact on near-surface chlorophyll stocks and oxygen supersaturation over the Campeche Canyon, Gulf of Mexico. J. Geophys. Res. Oceans 109, C05012, http://dx.doi.org/10.1029/2002JC001614.

Salas-de-León, D.A., Monreal-Gómez, M.A., Díaz-Flores, M.A., Salas-Monreal, D., Velasco-Mendoza, H., Riverón-Enzástiga, M.L., Ortiz-Zamora, G., 2008. Role of near-bottom currents in the distribution of sediments within the Southern Bay of Campeche, Gulf of México. J. Coastal Res. 24 (6), 1487—1494, http://dx.doi.org/10.2112/07-0857.1.

Salas-Monreal, D., Valle-Levinson, A., 2009. Continuously stratified flow dynamics over a hollow. J. Geophys. Res. Oceans 114 (C3), http://dx.doi.org/10.1029/2007JC004648.

Salas-Monreal, D., Salas-de-León, D.A., Monreal-Gómez, M.A., Riverón-Enzástiga, M.L., 2009. Current rectification in a tropical coral reef system. Coral Reefs 28 (4), 871—879, http://dx.doi.org/10.1007/s00338-009-0521-9.

Salas-Monreal, D., Salas-de-Leon, D.A., Monreal-Gomez, M.A., Riveron-Enzastiga, M.L., Mojica-Ramirez, E., 2012. Hydraulic jump in the Gulf of California. Open J. Mar. Sci. 2, 141—149, http://dx.doi.org/10.4236/ojms.2012.24017.

Scully, M.E., Geyer, W.R., Lerczak, J.A., 2009. The influence of lateral advection on the residual estuarine circulation: a numerical modeling study of the Hudson River estuary. J. Phys. Oceanogr. 39 (1), 107—124, http://dx.doi.org/10.1175/2008JPO3952.1.

Shanks, A.L., 1983. Surface slicks associated with tidally forced internal waves may transport pelagic larvae of benthic invertebrates and fishes shoreward. Mar. Ecol. Prog. Ser. 13 (2), 311—315.

Spiteri, C., Slomp, C.P., Tuncay, K., Meile, C., 2008. Modeling biogeochemical processes in subterranean estuaries: effect of flow dynamics and redox conditions on submarine groundwater discharge of nutrients. Water Resour. Res. 44 (2), W02430, http://dx.doi.org/10.1029/2007WR006071.

Storlazzi, C.D., Mc Manus, M.A., Logan, J.B., Mc Laughlin, B.E., 2006. Cross-shore velocity shear, eddies and heterogeneity in water column properties over fringing coral reefs: West Maui, Hawaii. Cont. Shelf Res. 26 (3), 401—421, http://dx.doi.org/10.1016/j.csr.2005.12.006.

Sutherland, D.A., MacCready, P., Banas, N.S., Smedstad, L.F., 2011. A model study of the Salish Sea Estuarine circulation. J. Phys. Oceanogr. 41 (6), 1125—1143, http://dx.doi.org/10.1175/2011JPO4540.1.

Valle-Levinson, A., Trasvina-Castro, A., Gutierrez-de-Velasco, G., Gonzalez-Armas, R., 2004. Diurnal vertical motions over a seamount of the southern Gulf of California. J. Mar. Syst. 50, 61—77.

Wang, J., Mysak, L.A., Ingram, R.G., 1994. A three-dimensional numerical simulation of Hudson Bay summer ocean circulation: topographic gyres, separations, and coastal jets. J. Phys. Oceanogr. 24 (12), 2496—2514, http://dx.doi.org/10.1175/1520-0485(1994)024<2496:ATDNSO>2.0.CO;2.

Wilkinson, C., Souter, D. (Eds.), 2008. Status of Caribbean Coral Reefs After Bleaching and Hurricanes in 2005. Global Coral Reef Monitoring Network, and Reef and Rainforest Research Centre, Townsville. 148 pp.

Xinyu, G., Valle-Levinson, A., 2007. Tidal effects on estuarine circulation and outflow plume in the Chesapeake Bay. Cont. Shelf Res. 27 (1), 20—42, http://dx.doi.org/10.1016/j.csr.2006.08.009.

Zeldis, J.R., Jillett, J.B., 1982. Aggregation of pelagic *Munida gregaria* (Fabricius) (Decapoda, Anomura) by coastal fronts and internal waves. J. Plankton Res. 4 (4), 839—857, http://dx.doi.org/10.1093/plankt/4.4.839.

Zhang, S., Zheng, G., Gao, H., Roelke, D., 2014. Satellite remote sensing of chlorophyll-*a* concentrations in the Galveston Bay, Texas. In: AGU Fall Meeting Abstracts 1. p. 232.